

Tuning and validation of hadronic event generator for R value measurements in the tau-charm region ^{*}

Rong-Gang Ping (平荣刚)¹ Xi-An Xiong (熊习安)¹ Lei Xia (夏磊)² Zhen Gao (高榛)²
 Ying-Tian Li (李应天)¹ Xing-Yu Zhou (周兴玉)¹ Bing-Xin Zhang (张丙新)¹ Bo Zheng (郑波)³
 Wen-Biao Yan (鄢文标)² Hai-Ming Hu (胡海明)¹ Guang-Shun Huang (黄光顺)²

¹Institute of High Energy Physics, Chinese Academy of Sciences, Beijing 100049, People's Republic of China

²University of Science and Technology of China, Hefei 230026, People's Republic of China

³University of South China, Hengyang, 421001, People's Republic of China

Abstract To measure the R value in an energy scan experiment with e^+e^- collisions, precise calculation of initial state radiation is required in the event generators. We present an event generator for this consideration, which incorporates initial state radiation effects up to second order accuracy. The radiative correction factor is calculated using the totally hadronic Born cross section. The measured exclusive processes are generated according to their cross sections, while the unknown processes are generated using the LUND Area Law model, and its parameters are tuned with data collected at $\sqrt{s} = 3.65$ GeV. The optimized values are validated with data in the range $\sqrt{s} = 2.2324 \sim 3.671$ GeV. These optimized parameters are universally valid for event generation below the $D\bar{D}$ threshold.

Key words Event generator, R value

PACS 13.66.Jn, 02.70.Uu

1 Introduction

The total cross section for hadron production in positron-electron (e^+e^-) annihilation is one of the most fundamental observables in particle physics. A precise measurement of the hadronic cross section allows us to determine the hadronic contributions to the running of the quantum electrodynamic (QED) fine structure constant α , electroweak parameters, and the strong coupling α_s . The R value, defined as the ratio of the total hadronic cross section to that of $e^+e^- \rightarrow \mu^+\mu^-$ at Born level, have been measured by many collaborations in e^+e^- scan experiments, over the center-of-mass energy from the two pion mass threshold ($M_{2\pi}$) to the Z peak [1]. In the tau-charm energy region, the R values measured at BESII [2] were used in the evaluation of the hadronic contribution from the five quark loops at the energy of Z peak, $\Delta\alpha_{\text{had}}^{(5)}(M_Z^2)$, with an improved precision by a factor of 2 [3].

A large number of exclusive processes have been measured over the range from $M_{2\pi}$ to 5 GeV [4], but most cross sections have large uncertainties. To improve these measurements, a hadronic event generator is needed for us to get better understanding of background events from $e^+e^- \rightarrow$ hadrons.

Especially, a precise R -value measurement requires excellent control of radiative correction (RC) and vacuum polarization (VP) in the Monte Carlo (MC) program. We design an event generator for measuring R values and exclusive decays in e^+e^- collisions. The generator is constructed in the framework of BesEvtGen [5], incorporating both the RC and VP effects. We also present details of the parameter optimization of the Lund Area Law (LUARLW) model [6] with data, and validations with various distributions within the energy range $\sqrt{s} = 2.2324 \sim 3.671$ GeV.

Received 31 June 2015

^{*} Supported by National Natural Science Foundation of China, under Contract NO. 11175146, 11375205, 11575077, 11335008, 11565006, Large Science Setup of Joint Foundation 10979059, and 100 Talents Program of CAS

1) E-mail: pingrg@ihep.ac.cn, zhengbo_usc@163.com

©2016 Chinese Physical Society and the Institute of High Energy Physics of the Chinese Academy of Sciences and the Institute of Modern Physics of the Chinese Academy of Sciences and IOP Publishing Ltd

2 Framework of event generator

The generator is constructed as a model of the BesEvtGen package. It provides the 4-momentum of each final state particle for detector simulation, and provides the ISR correction factor and VP factors for users to undress the observed cross section. The basic idea of this generator is to decompose the total hadronic cross section into the measured exclusive processes and remaining unknown processes. The latter are generated with the LUARLW model.

2.1 Initial state radiative correction

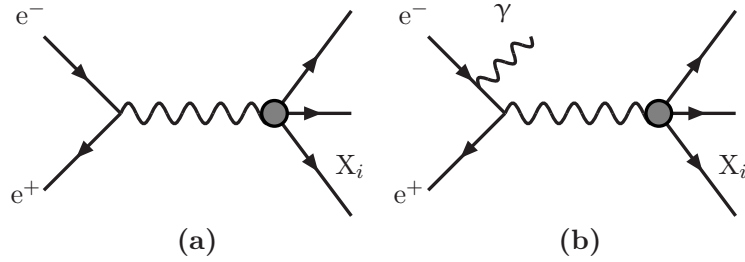


Fig. 1. Feynman diagrams for the process (a) $e^+e^- \rightarrow X_i$, and ISR process (b) $e^+e^- \rightarrow \gamma_{\text{ISR}}X_i$.

In an e^+e^- energy scan experiment, we consider a measurement of the Born cross section (σ_0) for a process $e^+e^- \rightarrow X_i$, as shown in Fig. 1 (a), where X_i denotes the hadron states of i -th process. Due to ISR, the observed cross section (σ) is actually for the process $e^+e^- \rightarrow \gamma_{\text{ISR}}X_i$, as shown in Fig. 1 (b). The observed cross section is related to the Born cross section by the quasi-real electron method [7]:

$$\sigma(s) = \int_{M_{\text{th}}}^{\sqrt{s}} dm \frac{2m}{s} W(s, x) \frac{\sigma_0(m)}{|1 - \Pi(m)|^2}, \quad (1)$$

where m is the invariant mass of the final states; $\Pi(m)$ is the vacuum polarization function, which will be discussed later; s is the e^+e^- center-of-mass energy squared; $x \equiv 2E_\gamma^*/\sqrt{s} = 1 - m^2/s$, and E_γ^* is the total energy carried by ISR photons in the e^+e^- center-of-mass frame; M_{th} is the mass threshold of a given process.

To calculate the finite-order leading logarithmic correction, the structure function method is used [8]. This method results in the same factorized form for the radiative photon emission cross section. Up to order α^2 , the radiative function takes the form:

$$W(s, x) = \Delta \beta x^{\beta-1} - \frac{\beta}{2}(2-x) + \frac{\beta^2}{8} \{ (2-x)[3\ln(1-x) - 4\ln x] - 4 \frac{\ln(1-x)}{x} - 6 + x \}, \quad (2)$$

where

$$L = 2 \ln \frac{\sqrt{s}}{m_e}, \quad (3)$$

$$\Delta = 1 + \frac{\alpha}{\pi} \left(\frac{3}{2}L + \frac{1}{3}\pi^2 - 2 \right) + \left(\frac{\alpha}{\pi} \right)^2 \delta_2, \quad (4)$$

$$\delta_2 = \left(\frac{9}{8} - 2\xi_2 \right) L^2 - \left(\frac{45}{16} - \frac{11}{2}\xi_2 - 3\xi_3 \right) L - \frac{6}{5}\xi_2^2 - \frac{9}{2}\xi_3 - 6\xi_2 \ln 2 + \frac{3}{8}\xi_2 + \frac{57}{12}, \quad (5)$$

$$\beta = \frac{2\alpha}{\pi}(L-1), \quad \xi_2 = 1.64493407, \quad \xi_3 = 1.2020569.$$

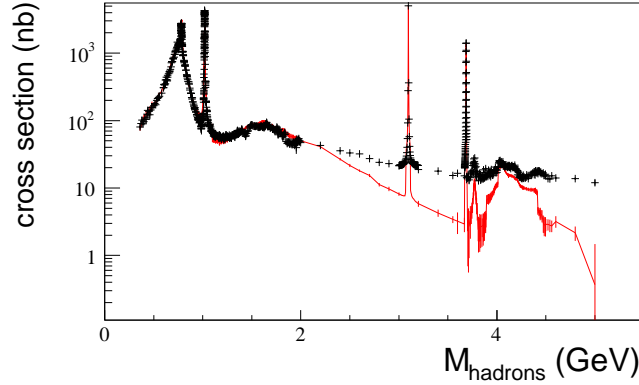


Fig. 2. (color online) The cross section for light hadron production within $M_{2\pi} \sim 5$ GeV, where the black points with errors are the total hadronic cross section [10], and the histogram with points (in red) is the sum of measured cross sections for exclusive processes.

Here the exponential part in Eq. (2) accounts for soft multi-photon emission, while the remaining part takes into account hard collinear bremsstrahlung in the leading logarithmic approximation. We use the radiative function up to the second order calculation to determine the cross section; it is accurate enough to construct the event generator for our purpose, though contributions from the α^3 -order are known [9].

To do the RC for the process $e^+e^- \rightarrow \text{hadrons}$, we use the cross sections for the light hadron productions measured so far. In the energy region from $M_{2\pi}$ to 5 GeV, the total cross sections are quoted from the Particle Data Group (PDG) [10]. The total distribution is shown in Fig. 2.

At the leading order of QED calculation, the ISR photon is characterized by soft energy and beam collinear distribution. A more general result is obtained by the method of Bonneau and Martin[11] up to m_e^2/s terms, and the angular distributions is calculated by

$$\frac{d\sigma(s, x)}{dx d\cos\theta} = \frac{2\alpha}{\pi x} \left(1 - x + \frac{x^2}{2}\right) \sigma_0(s(1-x)) P(\theta), \quad \text{with} \quad (6)$$

$$P(\theta) = \frac{\sin^2\theta - \frac{x^2 \sin^4\theta}{2(x^2 - 2x + 2)} - \frac{m_e^2}{E^2} \frac{(1-2x)\sin^2\theta - x^2 \cos^4\theta}{x^2 - 2x + 2}}{\left(\sin^2\theta + \frac{m_e^2}{E^2} \cos^2\theta\right)^2}, \quad (7)$$

where E is the beam energy in the center of mass system of the electron and positron.

2.2 Vacuum polarization

The VP of the photon is a quantum effect which leads to the scale dependence of the electromagnetic coupling. It therefore plays an important role in the e^+e^- physics and it is crucial to know it for the R value measurement.

Conventionally the VP function is denoted by $\Pi(q^2)$, where q is a space- or time-like momentum. In the R value measurement, we only consider the time-like case, i.e. $s = q^2$, which receives all possible one-particle irreducible leptonic and hadronic contributions. Their contributions to $\Pi(s)$ are calculated and then summed. While the leptonic contributions can be predicted within perturbative theory, the precise determination of the hadronic contributions depends on dispersion relations using experimental data as input.

The VP has been calculated by many groups and is available in the literature. Comparisons between them are given in Ref. [12]. There are notable differences below 1.6 GeV, and above 2.0 GeV; visible differences appear when approaching the charmonium resonances. We use the results from the Fred Jegerlehner group [13]. It provides leptonic and hadronic VPs both in

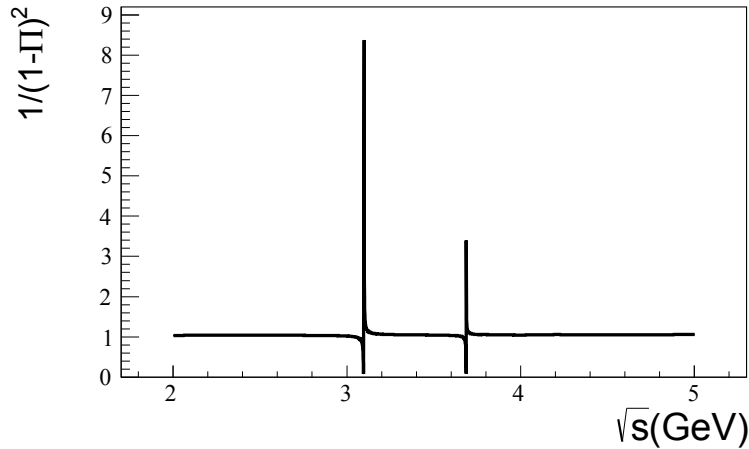


Fig. 3. Vacuum polarization factor $1/|1-\Pi(s)|^2$ quoted from Ref. [13].

the space- and time-like region. For the leptonic VP the complete one- and two-loop results and the known high-energy approximation for the three-loop corrections are included. The hadronic contributions are given in tabulated form in the subroutine HADR5N [14]. Figure 3 shows the VP factor defined by $1/|1-\Pi(s)|^2$ in the energy region $\sqrt{s}=2.0-5$ GeV. The values at J/ψ and $\psi(2S)$ peaks are very large but less significant elsewhere.

2.3 Cross sections for exclusive processes

Many exclusive processes have been measured in the e^+e^- collision experiments. Currently we collect 76 exclusive modes, with energy region covering from 0.3 GeV up to about 6 GeV. The Born cross sections are quoted from the published papers; their information is given in Table 1. The sum of these cross sections is shown in Fig. 2. Below 2.0 GeV, the total cross section is the sum of the exclusively measured ones.

The narrow vector resonances, such as $\psi(3770)$, $\psi(2S)$, J/ψ , $\rho(1700)$, and $\omega(1420)$, are also included in the calculation for the ISR correction factor. The cross sections for these narrow resonances are represented with the Breit-Wigner function

$$\sigma_{BW}(s) = 12\pi \frac{\gamma_{ee}\gamma}{(s - M^2) + M^2\gamma^2},$$

where M , γ , and γ_{ee} are the mass, total width and partial decay width to e^+e^- final state, respectively.

The distribution of cross section versus center-of-mass energy is described by an empirical function, which is parameterized with a multi-Gaussian function. Its parameters are determined by fitting the cross section mode by mode. These empirical functions are used in the generator for the calculation of the ISR correction factor and event type sampling.

The angular distribution for ISR photons is implemented according to Eq. (6). However, angular distributions are implemented only for two-body decays, namely, $1-\cos^2\theta$ for PP (where P is a pseudoscalar meson) modes, and $1+\alpha\cos^2\theta$ for the PV ($\alpha=1$) and $B\bar{B}$ modes, where V is a vector meson, and B is a baryon. The angular distribution parameter α for the $B\bar{B}$ mode is taken as the quark model prediction [43]. The phase space model is used for multi-body decays.

2.4 LUND Area Law model

The hadronic events produced in the e^+e^- annihilation are evolved as follows. As the first step, a quark-antiquark ($q\bar{q}$) pair is produced from a virtual photon, coupled to the e^+e^- pair. Then the $q\bar{q}$ branching proceeds via emitting gluons, and further develops into hadrons. In

Tab. 1. Collection of measured exclusive processes. Their cross sections are quoted from the references as given in table, together with the energy ranges.

ID	$e^+e^- \rightarrow$	\sqrt{s} (GeV)	Reference	ID	$e^+e^- \rightarrow$	\sqrt{s} (GeV)	Reference
1	$p\bar{p}$	1.877-4.500	[15]	39	$\omega\pi^+\pi^-$	1.150 - 2.525	[17]
2	$n\bar{n}$	1.90 - 2.44	[16]	40	$\omega f_0(980)$	1.700 - 2.475	[17]
3	$\Lambda\bar{\Lambda}$	2.23 - 5.00	[17]	41	$\eta'\pi^+\pi^-$	1.58 - 3.42	[17]
4	$\Sigma\bar{\Sigma}^0$	2.385 - 5.000	[17]	42	$f_1(1285)\pi^+\pi^-$	1.66 - 3.50	[17]
5	$\Lambda\bar{\Sigma}^0$	2.308 - 5.000	[17]	43	ωK^+K^-	1.57 - 3.45	[17]
6	$\Sigma^0\bar{\Lambda}$	2.308 - 5.000	[17]	44	$\omega\pi^+\pi^-\pi^0$	1.500 - 4.423	[21]
7	$\pi^+\pi^-$	0.305 - 2.950	[18]	45	$\Sigma^-\bar{\Sigma}^+$	2.308 - 5.000	[17]
8	$\pi^+\pi^-\pi^0$	1.063 - 2.989	[19]	46	K^+K^-	1.009 - 4.170	[27, 29]
9	$K^+K^-\pi^0$	1.34 - 4.68	[20]	47	$K_S K_L$	1.004 - 2.140	[27]
10	$K_S K^+\pi^-$	1.26 - 4.66	[20]	48	$\omega\eta$	1.371 - 3.178	[26]
11	$K_S K^-\pi^+$	1.26 - 4.66	[20]	49	$p\bar{p}\pi^0$	4.009 - 4.200	[28]
12	$K^+K^-\eta$	1.69 - 3.13	[20]	50	$p\bar{p}\eta$	4.009 - 4.200	[28]
13	$2(\pi^+\pi^-)$	0.615 - 4.45	[21]	51	$D^-D^{*0}\pi^+$	4.020 -5.171	[33]
14	$\pi^+\pi^-2\pi^0$	0.185 - 2.98	[22]	52	$D^+D^{*0}\pi^-$	4.020 -5.171	[33]
15	$K^+K^-\pi^+\pi^-$	1.425 - 4.988	[23]	53	$D^{*0}D^{*0}$	4.033 -4.991	[31]
16	$K^+K^-2\pi^0$	1.50 - 4.02	[23]	54	$D^0\bar{D}^{*0}$	4.033 -4.991	[30]
17	$2(K^+K^-)$	2.02 -4.54	[24]	55	\bar{D}^0D^{*0}	3.814 - 4.990	[30]
18	$2(\pi^+\pi^-)\pi^0$	1.013- 4.488	[25]	56	$D^0\bar{D}^0$	3.814 - 4.990	[30]
19	$2(\pi^+\pi^-)\eta$	1.313 - 4.488	[25]	57	D^+D^-	3.814 -4.990	[30]
20	$K^+K^-\pi^+\pi^-\pi^0$	1.613 - 4.488	[25]	58	D^+D^{*-}	3.890 -4.994	[31]
21	$K^+K^-\pi^+\pi^-\eta$	2.113 - 4.488	[25]	59	D^-D^{*+}	3.890 -4.994	[31]
22	$3(\pi^+\pi^-)$	1.313 - 4.488	[26]	60	$D^{*+}D^{*-}$	4.033 -4.991	[31]
23	$2(\pi^+\pi^-\pi^0)$	1.313 - 4.488	[26]	61	$D^0D^-\pi^+$	4.015 -4.974	[32]
24	$\phi\eta$	1.57 - 3.45	[20]	62	$\bar{D}^0D^+\pi^-$	4.015 -4.974	[32]
25	$\phi\pi^0$	1.25 - 1.45	[20]	63	$D^0D^{*-}\pi^+$	4.020 -5.171	[33]
26	K^+K^{*-}	1.37 -1.99	[20]	64	$\bar{D}^0D^{*+}\pi^-$	4.020 -5.171	[33]
27	K^-K^{*+}	1.37 - 1.99	[20]	65	$\psi(2S)\pi^0\pi^0$	4.127-5.480	[37]
28	$K_S\bar{K}^{*0}(892)$	1.37 - 1.99	[20]	66	$\eta J/\psi$	3.81 -4.68	[35]
29	$K^*(892)^0K^+\pi^-$	1.588 - 3.963	[23]	67	$\pi^+\pi^-\text{h}_c$	4.009-4.420	[38]
30	$K^*(892)^0K^-\pi^+$	1.588 - 3.963	[23]	68	$\pi^0\pi^0\text{h}_c$	4.009-4.420	[39]
31	$K^*(892)^-K^+\pi^0$	1.588 - 3.963	[23]	69	K^+K^-J/ψ	4.179 -4.970	[41]
32	$K^*(892)^+K^-\pi^0$	1.588 - 3.963	[23]	70	$K_S^0K_S^0J/\psi$	4.179 -4.970	[40]
33	$K_2^*(1430)^0K^+\pi^-$	2.348 - 3.965	[23]	71	$J/\psi\pi^+\pi^-$	3.829 -5.471	[36]
34	$K_2^*(1430)^0K^-\pi^+$	2.348- 3.965	[23]	72	$\psi(2S)\pi^+\pi^-$	4.127 -5.480	[37]
35	$K^+K^-\rho$	1.777 - 3.830	[23]	73	$D_s^+D_s^-$	3.97 -4.26	[42]
36	$\phi\pi^+\pi^-$	1.488 - 2.863	[23]	74	$D_s^{*+}D_s^-$	4.12 -4.26	[42]
37	$\phi f_0(980)$	1.888- 2.963	[23]	75	$D_s^{*-}D_s^+$	4.12 -4.26	[42]
38	$\eta\pi^+\pi^-$	1.025 - 2.975	[17]	76	$\Lambda_c^+\Lambda_c^-$	4.57 -4.64	[34]

the high energy region, the cluster model (e.g. HERWIG [44]) and LUND string model (e.g. JETSET/PYTHIA[45]) are available and precise enough to describe the hadronic fragmentation with parameters optimized at boson Z peak. However, in the intermediate and low energy region, parameters need to be optimized or a new model is desirable to describe the light quark fragmentation.

In the tau-charm energy region, the LUARLW model [6] has been proposed to estimate the multiplicity distribution for primary hadrons produced from the string fragmentation. The probability distribution reads:

$$P_n = \frac{\mu^n}{n!} \exp[c_0 + c_1(n - \mu) + c_2(n - \mu)^2], \quad (8)$$

with $\mu = \alpha + \beta \exp(\gamma\sqrt{s})$, where $c_0, c_1, c_2, \alpha, \beta$ and γ are parameters to be tuned with data. An interface to access the LUARLW model is designed in the BesEvtGen [5] framework, and is only used to generate the primary hadrons. The further decays into light hadrons are realized with BesEvtGen [5].

2.5 Monte Carlo algorithm

The event sampling proceeds via two steps. Firstly, the mass of the hadron system, M_{hadrons} , is sampled according to the distribution of the observed cross section, i.e. $d\sigma(s)/dm$, for the process $e^+e^- \rightarrow \gamma_{ISR} X_i$ according to Eq. (1). For simplicity, the ISR energy, $\sqrt{s} - M_{\text{hadrons}}$, is imposed on a single photon. The second step is to sample the event type topology according to the ratios of individual cross sections at the energy point M_{hadrons} .

2.5.1 Sampling of M_{hadrons}

To calculate the total observed cross section at \sqrt{s} , we split the integral of Eq. (1) into two parts, i.e.

$$\sigma(s) \equiv \sigma^I(s) + \sigma^{II}(s) = \int_{M_{\text{th}}}^{M_0} dm \frac{2m}{s} W(s, x) \frac{\sigma_0(m)}{|1 - \Pi(m)|^2} + \int_{M_0}^{\sqrt{s}} dm \frac{2m}{s} W(s, x) \frac{\sigma_0(m)}{|1 - \Pi(m)|^2}, \quad (9)$$

where the threshold energy M_{th} is the sum of masses for the final state particles, and the broken point is taken at $M_0 = \sqrt{s - 2\sqrt{s}E_\gamma^{\text{cut}}}$ with a cut E_γ^{cut} on the ISR photon energy. At the BESIII detector, the designed photon energy of the detection range is from ~ 20 MeV to 4.2 GeV [46]. If the photon energy is less than 20 MeV, it will be impossible to reconstruct it in the detection simulation. Hence in practice, E_γ^{cut} can be set to an energy less than the sensitivity of photon detection. e.g., $E_\gamma^{\text{cut}} = 1$ MeV. In the range $0 \sim E_\gamma^{\text{cut}}$, the ISR photon is too soft to be detected, so the ISR photon is not considered. To simplify the calculation, Born cross sections near the energy point \sqrt{s} are assumed to be a constant value $\sigma_0(\sqrt{s})$. Using the relation $x = 1 - m^2/s$, the second integral can be further decomposed into two parts:

$$\sigma^{II}(s) = \int_{M_0}^{\sqrt{s(1-b)}} dm \frac{2m}{s} W(s, x) \frac{\sigma_0(m)}{|1 - \Pi(m)|^2} + \frac{\sigma_0(\sqrt{s})}{|1 - \Pi(\sqrt{s})|^2} \lim_{a \rightarrow 0} \int_a^b W(s, x) dx, \quad (10)$$

with $b \ll 1$. Using the radiative function given in Eq. (2), one has

$$\begin{aligned} \lim_{a \rightarrow 0} \int_a^b W(s, x) dx &= \Delta b^\beta + \frac{\beta^2 b^2}{32} + \frac{\beta b^2}{4} - \frac{3}{16} \beta^2 b^2 \ln(1-b) + \frac{1}{4} \beta^2 b^2 \ln b - \frac{5}{16} \beta^2 b - \beta b \\ &+ \frac{3}{4} \beta^2 b \ln(1-b) - \beta^2 b \ln b - \frac{9}{16} \beta^2 \ln(1-b) + \frac{1}{2} \beta^2 \text{Li}_2(b), \end{aligned} \quad (11)$$

with Spence's function $\text{Li}_2(x) = -x + \frac{1}{4}x^2 - \frac{1}{9}x^3$ ($x \ll 1$).

To sample the M_{hadrons} , we split the region $M_{\text{th}} \sim \sqrt{s}$ into a few hundred intervals. The cumulative cross section up to the i -th interval, m_i , is

$$\hat{\sigma}(m_i) = \frac{1}{\sigma(s)} \int_{M_{\text{th}}}^{m_i} dm \frac{2m}{s} W(s, x) \frac{\sigma_0(m)}{|1 - \Pi(m)|^2}.$$

The M_{hadrons} is sampled according to the $\hat{\sigma}(m_i)$ distribution with the discrete MC sampling technique.

2.5.2 Sampling of event type

Using the discrete MC sampling technique, the final states for exclusive modes are sampled according to the ratios of their cross sections (σ_m) to the total cross section (σ^{tot}), i.e.,

$$c_m = \sigma_m(M_{\text{hadrons}}) / \sigma^{\text{tot}}(M_{\text{hadrons}}),$$

where m is an index for exclusive process, and events for the remainder part, $1 - \sum_m c_m$, are generated with the LUARLW model.

3 Optimization of LUARLW parameters

3.1 Strategy to optimize the LUARLW parameters

The LUARLW model parameters are optimized with the parameterized response function method. The optimal values are obtained by simultaneously fitting this function to data distributions. The idea for this method is borrowed from that implemented in the event generator tuning tool Professor and Rivet [47] system, which was introduced by TASSO, and later used by ALEPH, DELPHI [48–53], and recently by the LHC [47]. This method has the advantage of eliminating the problem from the so-called manual and brute-force tunings, such as the slow tuning procedure and the sub-optimal results.

An ensemble of MC samples was produced within the framework of the BesEvtGen [5] event generator, and then it is subject to detector simulation with BOSS software [57]. 91 independent MC samples were prepared, each one generated with a different set of LUARLW parameters, which were randomly chosen in the parameter space around a given central point \mathbf{p}_0 . All MC samples were produced with equal statistics, and were large enough so that the overall statistical uncertainties are negligible.

By including the correlations among the model parameters, the dependence of physical observable is expanded up to the quadratic term as done in Ref. [54], and the response function reads

$$\begin{aligned} f(\mathbf{p}_0 + \delta\mathbf{p}, x) &= a_0^{(0)}(x) + \sum_{i=1}^n a_i^{(1)}(x) \delta p_i \\ &+ \sum_{i=1}^n \sum_{j=i}^n a_{ij}^{(2)}(x) \delta p_i \delta p_j \approx MC(\mathbf{p}_0 + \delta\mathbf{p}, x), \end{aligned} \quad (12)$$

where n is the number of parameters to be fitted, and $MC(\mathbf{p}_0 + \delta\mathbf{p}, x)$ denotes the distribution of physical observable x predicted for a given set of parameter values $\mathbf{p}_0 + \delta\mathbf{p}$, where \mathbf{p}_0 is the central value and δp_i is the deviation of the i -th parameter. The quadratic term in the expansion accounts for the possible correlations between the model parameters. The number of coefficients $a^{(0,1,2)}$, L , in the expansion is calculated with

$$L = 1 + n + n(n+1)/2, \quad (13)$$

and the coefficients are determined by fitting Eq. (12) to the L reference simulation distributions. This fit is equivalent to solving a system of linear equations of Eq. (12). Then the optimal values of the parameters p_i , their errors σ_i , and their correlation coefficients ρ_{ij} will be determined with a standard χ^2 fit to data using package MINUIT [55]. The fit is done simultaneously for all distributions and for all bins.

To minimize statistical uncertainties, the model parameters should be fitted to the distributions that show strong dependence on the parameters under consideration and least dependence on the others. For each distribution, a quality to measure the sensitivity to the model i -th parameter is calculated, i.e.

$$S_i(x) = \frac{\delta MC(x)}{MC(x)} \Big|_{p_i} / \frac{\delta p_i}{p_i} \approx \frac{\partial \ln MC(x)}{\partial \ln |p_i|} \Big|_{p_i}, \quad (14)$$

where $\delta MC(x)$ is the change of the distribution $MC(x)$ when the model parameter p_i is changed by δp_i from its central value. Sensitivity values for charged track distributions and event shapes vary within the range from -0.3 to 0.3, but the polar angle and azimuthal distributions for charged tracks are not sensitive to the change of model parameters. This is because the inclusive charged tracks are distributed isotropically over the whole phase space. Taking the sensitivity into consideration, only 12 observable distributions are kept for the model parameter fit. They are the number of photons (N_γ), the number of charged tracks (N_{track}), momentum of tracks (P_{track}), $x_f = 2P_z/W$, $x_\perp = 2P_\perp/2W$, sphericity, aplanarity, thrust, oblateness, and Fox-Wolfram moments (H_{20}, H_{30}, H_{40}) [45], where W is the total reconstructed energy of an event, and P_\perp is the transverse momentum.

We have 12 parameters to be optimized. According to Eq. (13), there are 91 coefficients, $a^{(0,1,2)}$ in Eq. (12) to be determined. Hence we need at least 91 MC samples to determine these coefficients. These were prepared with 0.5 million events for each sample. Then the dependence of response function on model parameters is established, and this analytical expression is used to simultaneously fit to the data distributions after QED background events are subtracted. In the optimization procedure, the χ^2 function is defined over each bin, i.e., $\chi^2 \rightarrow \chi^2/N$, where χ^2 values are calculated over nonempty N bins. To consider the requirement of fit goodness on the multiplicity of charged tracks, this distribution is weighted with a factor of 10, while other distributions are weighted with a unitary factor. This weighted factor is chosen by requiring that the fit quality of all distributions are satisfactory.

3.2 Event selection and fit results

We use the data taken at $\sqrt{s} = 3.65$ GeV to optimize the parameters. To validate these parameters, we check whether it is suitable for describing the data distribution in the energy region 2.0 – 4.26 GeV. The QED backgrounds, e.g. $e^+e^- \rightarrow e^+e^-$, $\gamma\gamma$, $\gamma^*\gamma^*$, $\mu^+\mu^-$, and $\tau^+\tau^-$ are subtracted using MC samples, and they are normalized according to their cross sections to the luminosity of data sets. The event selection criteria for light hadrons are similar to those applied to the R value measurements [2, 56].

The selected candidates are characterized by the distributions of charged track multiplicity (N_{track}), track energy (E_{track}) and momentum (p_{track}), polar angle ($\cos\theta$), azimuthal angle (ϕ), rapidity, pseudorapidity, and a set of event shapes. These distributions are normalized to one and the errors are scaled for all bins.

To consider the possible correlations between these observable quantities, different observable combinations were tried. In each combination, track observables, N_γ , N_{track} , E_{track} , x_f and x_\perp , must be included, while the p_{track} distribution or event shapes are partly included in the simultaneous fit. Generally speaking, the more observable distributions are involved in the fit, the worse fit quality one gets. To validate the resulted parameters, they are reused to generate

Tab. 2. Optimized parameters at $\sqrt{s}=3.65$ GeV. The statistical errors are negligible. $^{(2S+1)}P_J$ denotes a meson has spin S , orbital angular momentum (L) and total spin J .

Parameters	Tuned	Description
PARJ(1)	0.065	Suppression of diquark-antidiquark pair production
PARJ(2)	0.260	Suppression of s quark pair production
PARJ(11)	0.612	Probability that a light meson has spin 1
PARJ(12)	0.000	Probability that a strange meson has spin 1
PARJ(14)	0.244	Probability for a 1P_1 meson production
PARJ(15)	0.000	Probability for a 3P_0 meson production
PARJ(16)	0.437	Probability for a 3P_1 meson production
PARJ(17)	0.531	Probability for a 3P_2 meson production
PARJ(21)	0.066	Width of Gaussian for transverse momentum
RALPA(15)	0.577	LUARLW model parameter
RALPA(16)	0.364	LUARLW model parameter
RALPA(17)	0.000	LUARLW model parameter

MC samples, and compared to data.

The covariant matrix in fitting was checked, and it shows that there are strong correlations among these parameters. This indicates that the model parameters in question are not independent, which leads to some technical issues. One is the instability of the fitted values. If initial values are changed, then the fit gives a different set of parameters with almost the same fit quality. The dependence on the initial values brings about the so called multi-solution. Fortunately, we find that the produced MC distributions with these multi-solution values are in good agreement with data distributions. The correlation between the parameters means that the fitted value may be unphysical. One recipe to tackle this issue is to fix correlated parameters to the physical values, thus the fit can yield physical values for uncorrelated model parameters.

4 Validation of tuned parameters

In the simultaneous fit to data, we have tried various combination of data distributions, which results in a few sets of parameters. To select the most optimal values, we compare the data to the MC distributions, which are generated with optimized parameters for all sets. We require that the parameters can produce MC distributions having the best fit goodness quality χ^2/N , where N is the total number of bins for calculating the χ^2 values. The optimal values are given in Table 2. These values are only responsible for unknown processes other than the exclusive modes. For example, the parameter PARJ(15)=0 implies that exclusive modes have produce sufficient scalar mesons, so the LUARLW model forbids the scalar meson production.

Figure 4 shows a comparison of data and MC distributions at $\sqrt{s} = 3.65$ GeV, where the MC sample is produced with the optimized parameters. The agreement between them is satisfactory. To demonstrate the flexibility of these parameters at low energy points, we generate MC at 3.06 GeV with the same parameters, and Fig. 5 shows comparisons between the data and MC simulation. The agreement between the data and MC distributions is acceptable. However, above the $D\bar{D}$ threshold, we check these parameters with the data taken at 4.26, 4.23 and 4.6 GeV, and we find that the agreement between data and MC gets worse. This suggests that the optimized parameters are acceptable only below the $D\bar{D}$ threshold. To optimize parameters above the $D\bar{D}$ threshold, the charm meson decays will have to be added.

To validate this set of parameters for the MC generation below the $D\bar{D}$ threshold, we compare the charged track multiplicity distributions at 14 energy points from $\sqrt{s} = 2.2324$ to 3.671 GeV, as shown in Fig. 6. When extending this set of parameters from 3.65 GeV to low energy points, the agreement between the data and MC multiplicity distributions gets better. This is due to the fact that the total cross section equals the sum of the exclusive ones when approaching the energy 2.0 GeV, as shown in Fig. 2.

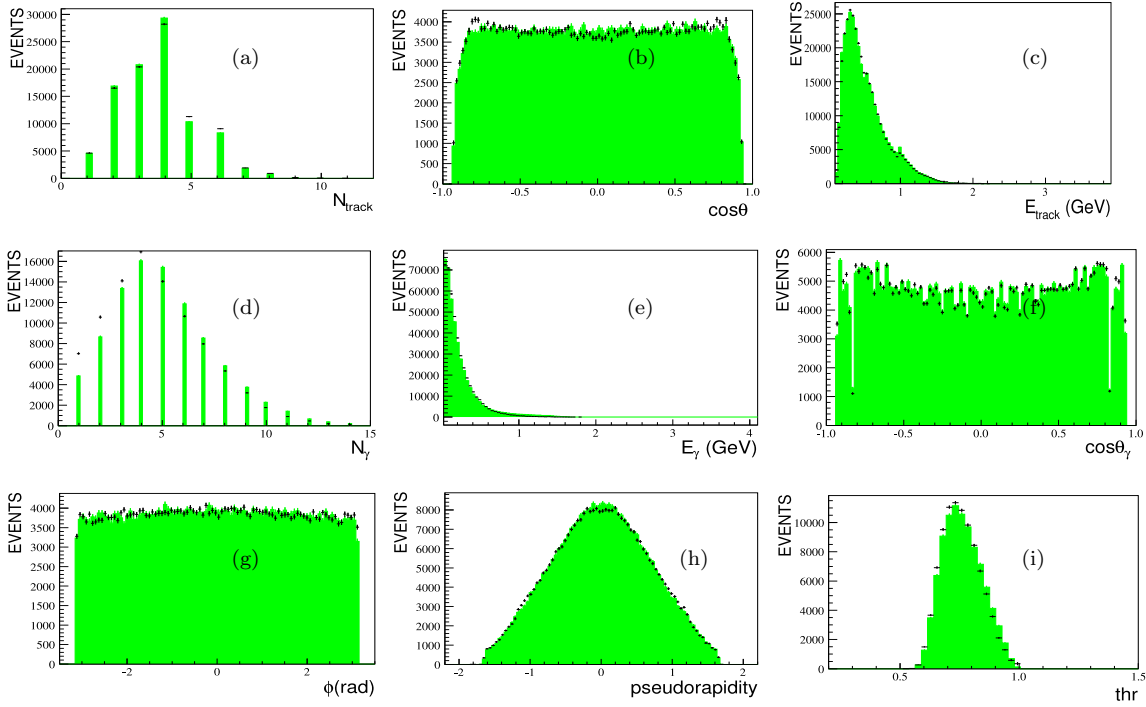


Fig. 4. (color online) Comparison of data to MC distributions at 3.65 GeV, where the MC sample is produced with the optimized parameters: (a) multiplicity of charged tracks, (b) cosine of polar angle of charged tracks, (c) energy of charged tracks, (d) multiplicity of photon, (e) energy of photon, (f) cosine of polar angle of photons, (g) azimuthal distribution, (h) pseudorapidity and (i) thrust. Where the points with errors are data, and shaded histogram is MC distribution.

5 Discussion and summary

To summarize, we have developed an event generator for R measurement at energy scan experiments, incorporating the initial state radiation effects up to the second order correction. In the event generator, the ISR correction factor is calculated using the totally hadronic Born cross sections measured in experiments. The measured exclusive processes are generated according to their cross sections, while unknown processes are generated using the LUARLW model, whose parameters are tuned with the data collected at 3.65 GeV. To validate the optimized parameters, we compare various distributions using data sets covering from energy $\sqrt{s} = 2.2324$ to 3.671 GeV. We conclude that the optimized parameters are valid for MC generation below the $D\bar{D}$ threshold. Above the $D\bar{D}$ threshold, the parameters should be optimized with the charm meson decays.

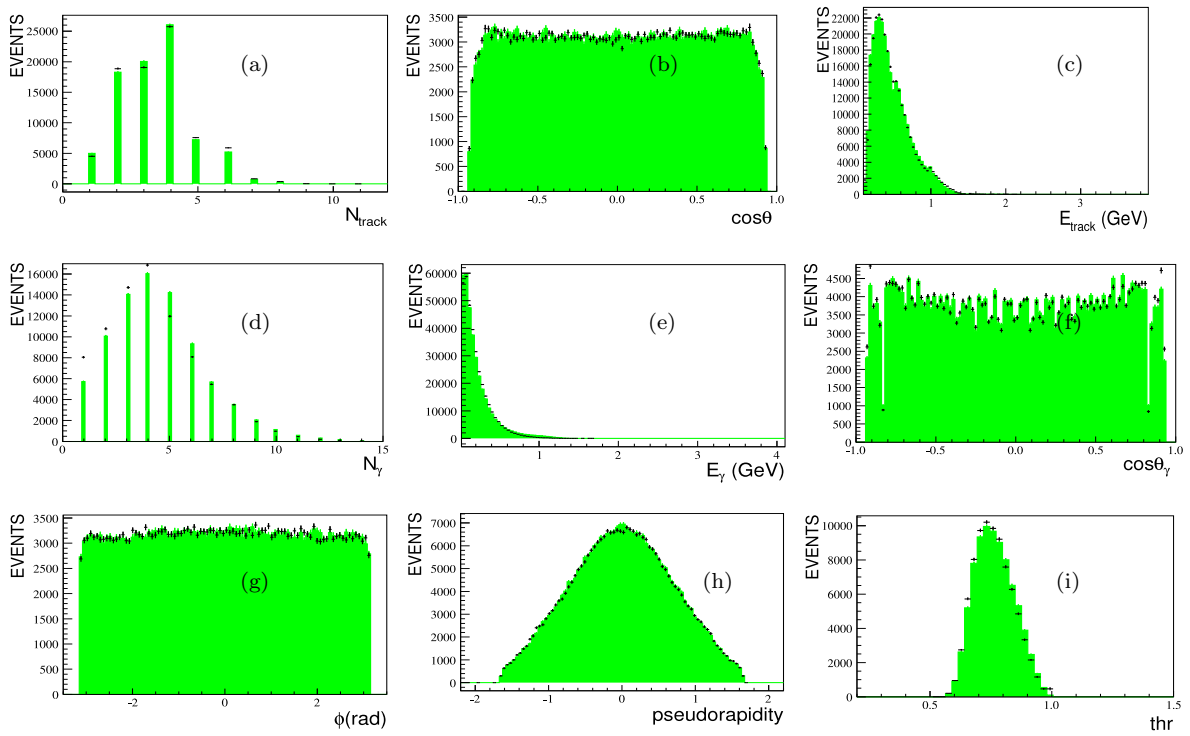


Fig. 5. (color online) Comparison of data to the MC distributions at 3.06 GeV, where the MC sample is produced with the optimized parameters: (a) multiplicity of charged tracks, (b) cosine of polar angle of charged tracks, (c) energy of charged tracks, (d) multiplicity of photon, (e) energy of photon, (f) cosine of polar angle of photons, (g) azimuthal distribution, (h) pseudorapidity and (i) thrust. Where the points with errors are data, and shaded histogram is MC distribution.

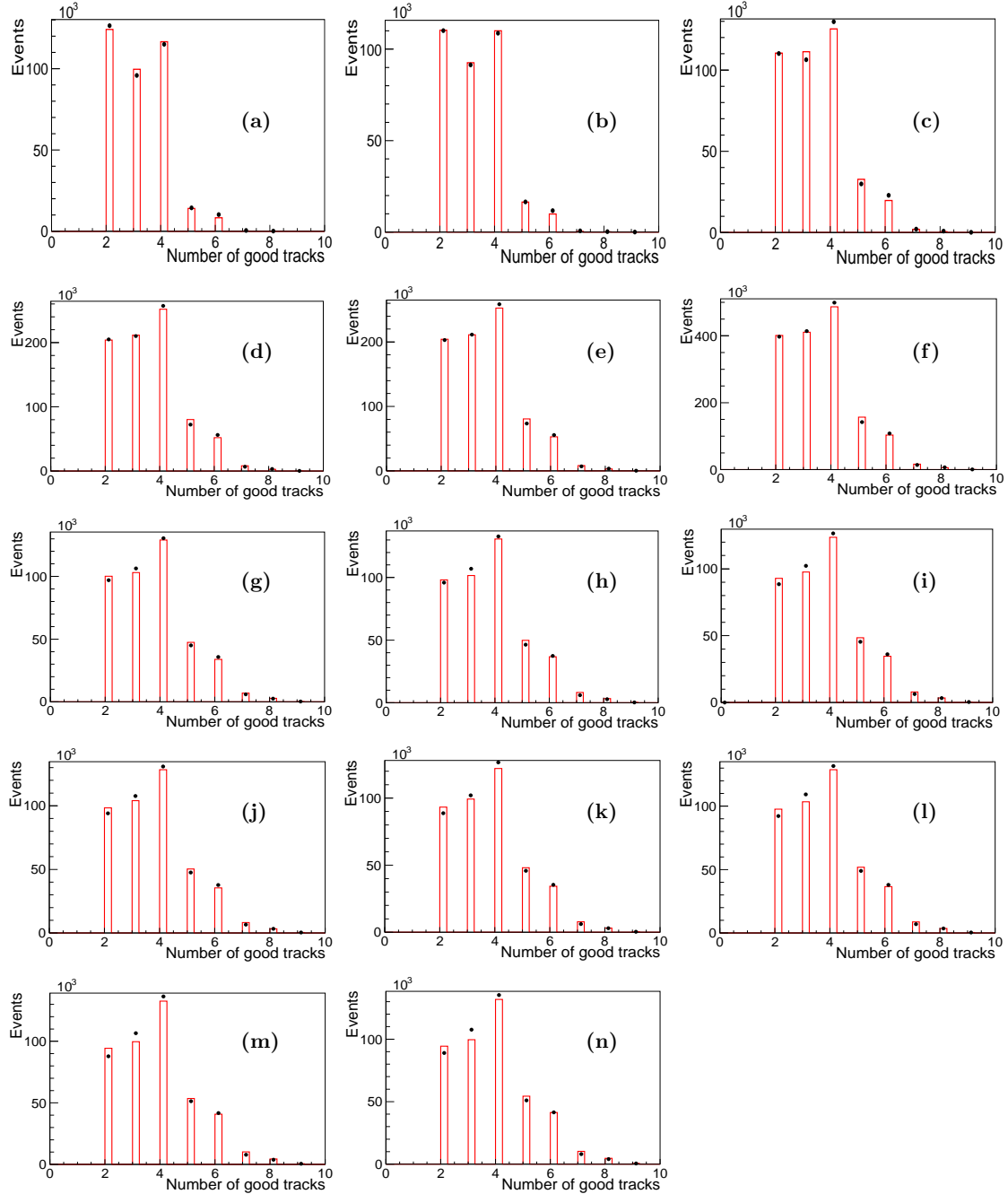


Fig. 6. (color online) Comparison of distributions between data and MC for the number of charged tracks at (a) 2.2324 GeV, (b) 2.4000 GeV, (c) 2.8000 GeV, (d) 3.0500 GeV, (e) 3.0600 GeV, (f) 3.0800 GeV, (g) 3.400 GeV, (h) 3.500 GeV, (i) 3.5424 GeV, (j) 3.5538 GeV, (k) 3.5611 GeV, (l) 3.6002 GeV, (m) 3.6500 GeV, (n) 3.6710 GeV. The dots denote data, and the open bars denote MC.

We are grateful to Prof. Yuan Changzheng, Prof. Li Haibo, Dr. Zhu Kai and Dr. Wang Yaqian for valuable suggestions on the text revision

References

- 1 For the most recent reviews, see, for example: B. Pietrzyk, Nucl. Phys. B (Pro. Suppl.), **162**: 18, (2006); F. Jegerlehner, Nucl. Phys. B (Pro. Suppl.), **162**:22, (2006) [hep-ph/0608329]; F. Ambrosino et al, Eur. Phys. J. C, **50**: 729, (2007) [hep-ex/0603056].
- 2 J. Z. Bai et al(BES Collaboration), Phy. Rev. Lett. **88**: 101802, (2002) [hep-ex/0102003].
- 3 H. Burkhardt and B. Pietrzyk, Phys. Lett., **B513**: 46, (2001); F. Jegerlehner, J. Phys. G, **29**: 101, (2003).
- 4 V. P. Druzhinin et al, Rev. Mod. Phys., **83**: 1545, (2011); M. R. Whalley, J. Phys. G, **29**: A1 (2003).
- 5 R. G. Ping, Chin. Phys. C, **32**: 599, (2008).
- 6 Kuang-Ta Zhao and Yifang Wang, Int. J. Mod. Phys. A, **24**, Supp. 1 (2009); Bo Andersson and Haiming Hu, arXiv:hep-ph/9910285; Haiming Hu and An Tai, arXiv:hep-ex/0106017.
- 7 V. N. Baier and V. S. Khoze, Nucl. Phys. B, **65**: 381, (1973); D. R. Yennie, S. C. Frautschi, H. Suura, Ann. Phys., **13**: 379, (1961).
- 8 E. A. Kuraev and V. S. Fadin, Sov. J. Nucl. Phys., **41**: 466, (1985).
- 9 G. Montagna, O. Nicrosini, F. Piccinini, Phys. Lett. B, **406**: 243, (1997).
- 10 K. A. Olive, et al, Chin. Phys. C, **38**: 1, (2014).
- 11 G. Bonneau and F. Martin, Nucl. Phys. B, **27**: 381, (1971).
- 12 S. Actis, et al, Eur. Phys. J. C, **66**: 585, (2010).
- 13 S. Eidelman, F. Jegerlehner, Z. Phys. C, **67**: 585 (1995) [hep-ph/ 9502298]; F. Jegerlehner, Nucl. Phys. Proc. Suppl., **162**: 22 (2006) [hep-ph/ 0608329]; F. Jegerlehner, Nucl. Phys. Proc. Suppl., **135**: 181, (2008); F. Jegerlehner, Nucl. Phys. Proc. Suppl., **126**: 325, (2004) [hep-ph/ 0310234]; F. Jegerlehner, hep-ph/0308117 (2003).
- 14 The full set of routines can be downloaded from Jegerlehner' s web page <http://www-com.physik.hu-berlin.de/~fjeger/>.
- 15 B. Aubert et al (Babar Collaboration), Phys. Rev. D, **73**: 012005, (2006).
- 16 A. Anotnelli et al, Nucl. Phys. B, **517**: 3, (1998).
- 17 B. Aubert et al (Babar Collaboration), Phys. Rev. D, **76**: 092005, (2007).
- 18 J. P. Lees et al (Babar Collaboration), Phys. Rev. D, **86**: 032013, (2012).
- 19 B. Aubert et al (Babar Collaboration), Phys. Rev. D, **70**: 072004, (2004).
- 20 B. Aubert et al (Babar Collaboration), Phys. Rev. D, **77**: 092002, (2008) .
- 21 B. Aubert et al (Babar Collaboration), Phys. Rev. D, **71**: 052001, (2005).
- 22 V. P. Druzhinin (Babar Collaboration), arXiv:0710.3455.
- 23 J. P. Lees et al (Babar Collaboration), arXiv:1103.3001.
- 24 B. Aubert et al (Babar Collaboration), Phys. Rev. D, **76**: 012008, (2007).
- 25 B. Aubert et al (Babar Collaboration), Phys. Rev. D, **76**: 092005, (2007).
- 26 B. Aubert et al (Babar Collaboration), Phys. Rev. D, **73**: 052003, (2007).
- 27 M. R. Whalley, J. Phys. G, **29**:A1 (2003).
- 28 Jie Liu, PHD thesis, (2015).
- 29 T. K. Pedlar et al (CLEO Collaboration), Phys. Rev. Lett., **95**: 261803, (2005); Kamal K Seth et al, arXiv: 1210.1596.
- 30 G. Pakhlova et al (Belle Collaboration), Phys. Rev. D, **77**: 011103, (2008).
- 31 G. Pakhlova et al (Belle Collaboration), Phys. Rev. Lett., **98**: 092001, (2007) [arXiv: hep-ex/0608018].
- 32 G. Pakhlova et al (Belle Collaboration), Phys.Rev.Lett., **100**: 062001, (2008) [arXiv: 0708.0082].
- 33 G. Pakhlova et al (Belle Collaboration), Phys. Rev. D, **80**: 091101, (2009) [arXiv: 0908.0231]
- 34 G. Pakhlova et al (Belle Collaboration), Phys. Rev. Lett., **101**: 172001, (2008) [arXiv: 0807.4458].
- 35 X. L. Wang et al Belle Collaboration, Phys. Rev. D, **87**: 051101, (2013);
- 36 C. Z. Yuan et al (Belle Collaboration), Phys. Rev. Lett., **99**: 182004, (2007) [arXiv:0707.2541].
- 37 X. L. Wang et al (Belle Collaboration), Phys. Rev. Lett., **99**:142002, (2007) [arXiv:0707.3699].
- 38 M. Ablikim et al (BESIII Collaboration),Phys. Rev. Lett. **111**:242001, (2013).
- 39 M. Ablikim et al (BESIII Collaboration),Phys. Rev. Lett. **113**:212002, (2014).
- 40 C.Z.Yuan et al (Belle Collaboration),Phys. Rev. D **77**: 011105, (2008); arXiv: 0709.2565.
- 41 C. Z. Yuan et al (Belle), Phys. Rev. D, **77**: 011105, (2008) [arXiv: 0709.2565].
- 42 D. Cronin-Hennessy et al (CLEO Collaboration), Phys. Rev. D, **80**: 072001, (2009).
- 43 Pang Cai-Yun and Ping Rong-Gang, Chin. Phys. Letts., **24**: 1411 (2007).
- 44 M. Bahr et al, Eur. Phys. J. C, **58**: 639, (2008).
- 45 T. Sjostrand, S. Mrenna, P. Skands, J. High Energy Phys., **0605**: 026, (2006) [hep-ph/0603175].
- 46 M. Ablikim et al Nucl. Instrum. Meth. A **614**: 345, (2010).
- 47 A. Buckley, H. Hoeth, H. Lacker et al, Eur. Phys. J. C, **65**: 331, (2010).
- 48 M. Althoff et al. (TASSO Collaboration), Z. Phys. C, **26**: 157, (1984).
- 49 W. Braunschweig et al. (TASSO Collaboration), Z. Phys. C, **41**: 359, (1988).
- 50 D. Buskulic et al. (ALEPH Collaboration), Z. Phys. C, **55**: 209, (1992).
- 51 R. Barate et al. (ALEPH Collaboration), Phys. Rep., **294**: 1, (1998).
- 52 K. Hamacher, M. Weierstall, hep-ex/9511011, (1995).
- 53 P. Abreu et al (DELPHI Collaboration), Z. Phys. C, **73**: 11, (1996).
- 54 P. Abreu, W. Adam, T. Auye et al, Z. Phys. C, **73**: 11, (1996).
- 55 F. James, CERN-D-506 CERN-D506, (1994); F. James and M. Roos, Comput. Phys. Commun., **10**: 343, (1975).
- 56 M. Ablikim et al., Phys. Lett. B, **677**: 239, (2009) .
- 57 Z. Y. Deng et al., High Energy Physics and Nuclear Physics, **30**: 371, (2006).
- 58 S. Jadach, B. F. L. Ward , and Z. Was, Phys. Rev. D, **63**: 113009, (2001); B. F. L. Ward, S. Jadach, and Z. Was, Nucl. Phys. B, Proc. Suppl. **116**:73, (2003).
- 59 Piotr Golonka and Zbigniew Was, Eur. Phys. J. C, **45**:97, (2006).